iScience

Article

m276-SL-PBD eradicates tumors and instigates long-lasting tumor-free survival in Merkel cell carcinoma preclinical models

Graphical abstract

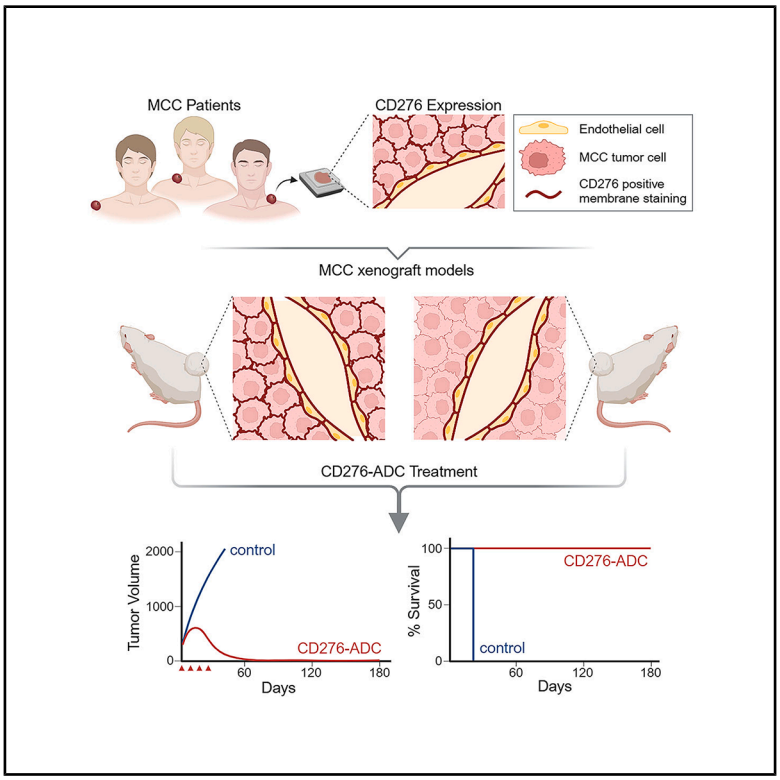

Authors

Mikaela D. Kunika, Aarthi Kannan, Graham J. Velasco, ..., Haibo Zhao, Brad St. Croix, Ling Gao

Correspondence

ling.gao@va.gov

In brief

Therapeutic procedure; Biotechnology; Cancer

Highlights

- CD276 is frequently overexpressed in MCC patient tumor cells and tumor vasculature
- CD276-ADC (m276-SL-PBD) eradicates MCC xenograft tumors, inducing long-term survival
- m276-SL-PBD remains highly effective in relapsed MCC xenograft tumors
- m276-SL-PBD specifically targets tumors in humanized mice, sparing human immune cells

Kunika et al., 2025, iScience *28*, 112436
May 16, 2025
https://doi.org/10.1016/j.isci.2025.112436

CellPress

iScience

CellPress
OPEN ACCESS

Article

m276-SL-PBD eradicates tumors and instigates long-lasting tumor-free survival in Merkel cell carcinoma preclinical models

Mikaela D. Kunika,[1] Aarthi Kannan,[1,4] Graham J. Velasco,[2] Yang Feng,[3] Steven Seaman,[3] Bhaba K. Das,[1] Dillon Pham,[1] Nils Lambrecht,[2] Haibo Zhao,[1] Brad St. Croix,[3] and Ling Gao[1,4,5,6,*]

[1]Southern California Institute for Research and Education, Long Beach, CA 90822, USA
[2]Pathology Department, Tibor Rubin VA Medical Center, VA Long Beach Healthcare System, Long Beach, CA 90822, USA
[3]Tumor Angiogenesis Unit, Mouse Cancer Genetics Program (MCGP), National Cancer Institute (NCI), NIH, Frederick, MD 21702, USA
[4]Department of Dermatology, University of California-Irvine, Irvine, CA 92697, USA
[5]Dermatology Section, Tibor Rubin VA Medical Center, VA Long Beach Healthcare System, Long Beach, CA 90822, USA
[6]Lead contact
*Correspondence: ling.gao@va.gov
https://doi.org/10.1016/j.isci.2025.112436

SUMMARY

Merkel cell carcinoma (MCC) is a rare but aggressive neuroendocrine carcinoma, and immune checkpoint inhibitors (ICIs) are the only approved therapy; nonetheless, resistance is notable and there is a critical need for novel effective therapies. Recently, CD276 was identified as a promising therapeutic target in human cancers. In preclinical studies, a modified CD276 antibody-drug conjugate (ADC) with pyrrolobenzodiazepine (m276-SL-PBD) elicited more potent anti-tumor effects than two CD276 ADCs currently in clinical trials. Here, we uncover notable CD276 expression in MCC patient tumors, and demonstrate m276-SL-PBD efficacy against MCC preclinical models. Complete eradication is observed in all xenografts bearing CD276 expression, with 82% achieving 180-day tumor-free survival after 4 or 5 weekly doses, and m276-SL-PBD remained efficacious against relapsed tumors. Of clinical relevance, m276-SL-PBD retains its potency in MCC-bearing humanized mice. Importantly, no detectable adverse effects were observed. Thus, m276-SL-PBD is a promising therapy for patients unsuitable or resistant to ICIs.

INTRODUCTION

Merkel cell carcinoma (MCC) is a rare but aggressive neuroendocrine carcinoma of the skin with increasing incidence and high mortality rates.[1–5] Since the discovery of Merkel cell polyomavirus (MCPyV) in 2008, MCC has been classified as either MCPyV-positive or MCPyV-negative.[4,6–8] Despite differing etiologies, both groups exhibit comparable clinical manifestations and prognoses.[9] While immune checkpoint inhibitors (ICIs) have shown durable response rates in eligible patients and remain the only Food and Drug Administration (FDA)-approved drugs for advanced MCC, a significant portion of these patients are intrinsically resistant or develop acquired resistance.[10–14] Furthermore, approximately half of MCC patients are ineligible for ICIs due to comorbidities.[11,15] Thus, effective treatment options remain in high demand for MCC patients, underscoring an urgent need to explore alternatives.

Antibody-drug conjugates (ADCs) have emerged as a promising therapeutic strategy for advanced cancers and offer an appealing alternative to ICIs. These agents are capable of delivering potent cytotoxic drugs directly to antigens expressed on tumor cells or cells in the tumor microenvironment (TME), thereby minimizing systemic drug exposure and associated toxicity.[16–19] There are currently thirteen FDA-approved ADCs for hematological malignancies and solid tumors.[17,20] Two ADCs targeting CD56[21] have been evaluated in MCC preclinical studies and early phase clinical trials, respectively.[22–25] Adcitmer, a CD56-targeting ADC conjugated to monomethyl auristatin E (MMAE), only delayed MCC xenograft tumor growth without achieving complete response.[22] While IMGN901, a CD56-targeting ADC with the cytotoxic payload maytansinoid DM1, showed objective responses in 3 of 23 metastatic MCC patients (NCT00346385),[24] a subsequent phase II study in small cell lung cancer patients resulted in unacceptable toxicity, leading to discontinuation.[26] Thus, there remains a need for more effective targets for antibody-based therapies in MCC.

CD276 (B7-H3), an immunomodulatory molecule of the B7 superfamily,[27] is frequently overexpressed in human cancers,[28–30] with studies showing that CD276 overexpression is associated with poor prognosis and metastasis,[28–31] making it an attractive target for antibody-based therapeutic strategies, including ADCs.[32] Currently, two CD276-targeting ADCs, MGC018 (NCT05551117/NCT06227546) and DS-7300a (NCT05280470/NCT06330064) are in phase II trials, indicating that targeting CD276 is safe. Seaman et al.[18] first developed m276-glyco-PBD, a pyrrolobenzodiazepine (PBD)-conjugated CD276-ADC,

which exhibited potent anti-tumor effects against several human cancers in preclinical studies. They recently developed a modified version, m276-SL-PBD, with improved drug conjugation and reduced off-target effects, which demonstrated even more potent preclinical anti-tumor efficacy.[33,34] The distinctive feature of m276-SL-PBD is its ability to target both tumor cells and tumor vasculature; by targeting tumor vasculature, m276-SL-PBD leverages a more mutation-resistant target, minimizing the development of drug resistance and inhibiting metastasis.[18] Notably, m276-glyco-PBD[18] and its successor m276-SL-PBD[33,34] have demonstrated superior potency surpassing outcomes reported in preclinical studies for Adcitmer,[22] MGC018,[35] and DS-7300a.[36] Additionally, the immunoglobulin G1 antibody, m276, utilized in m276-SL-PBD has similar binding affinity to both murine and human CD276, making it particularly suitable for preclinical evaluation in a murine TME.[18]

In this study, we found high CD276 expression in tumor cells and tumor vasculature in 83 of 84 MCC patient tumors, as well as in primary MCC cell lines and patient-derived xenografts (PDXs), supporting CD276 as a potential therapeutic target in MCC. Consistent with our hypothesis, m276-SL-PBD elicited potent and durable anti-tumor activity in both MCC cell line-derived (CDX) and patient-derived (PDX) mouse models, independent of MCPyV status. All xenografts with CD276 expression in tumor cells and/or tumor vasculature achieved complete response after initial treatment (48/48), with 82% remaining tumor-free to the 180-day experimental endpoint. Of note, in the CDX model derived from MCC-5 tumor cells with minimal CD276 expression, high CD276 expression was detected in tumor-associated murine vasculature; m276-SL-PBD still led to complete eradication of xenografts, likely through its reactivity with CD276-expressing tumor vasculature. With high clinical relevance, this study represents the first application of humanized mice in the MCC preclinical setting, providing a model that better reflects patient TME for evaluating drug efficacy and side effect. Furthermore, m276-SL-PBD retained its efficacy against relapsed tumors with sustained CD276 expression. These findings have provided compelling evidence for m276-SL-PBD as a novel therapy for MCC patients.

RESULTS

CD276 is expressed in primary MCC cell lines and PDXs

CD276 overexpression in tumor cells and tumor vasculature has been linked to recurrence, metastasis, and poor prognosis across various human cancers.[27,29,30,37,38] A prior study[37] first examined CD276 expression in MCC patient tumors, reporting low frequency of CD276 expression in tumor cells and strong expression exclusively in tumor vasculature. To investigate CD276 expression in tumor cells, we utilized multiple primary MCC cell lines (STAR Methods) to examine CD276 expression at both transcript and protein levels. MCC-5, MCC-9, and MCC-22 are MCPyV-negative, while MCC-16, MCC-21, and MKL-1 are MCPyV-positive. Variable CD276 expression was detected across all six cell lines, independent of MCPyV status (Figures 1A and 1B), suggesting that CD276 is a potential therapeutic target for a broad cohort of MCC patients. MCC-9 and MKL-1 exhibited the highest CD276 levels, while MCC-5 showed extremely low *CD276* mRNA expression and was almost undetectable at the protein level. Additionally, we examined CD276 expression in two PDX lineages established and characterized in our laboratory (STAR Methods), MCPyV-negative PDX-104 and MCPyV-positive PDX-60 from respective MCC patients (Table S1), both of which displayed high CD276 expression (Figure 1B). Thus, we have confirmed that CD276 was variably expressed in MCC tumor cells, independent of MCPyV status.

CD276 is highly expressed in MCC patient tumors and tumor vasculatures

To further validate our findings, we examined CD276 expression in 84 archival MCC patient tumors (Table S2), using the anti-CD276 antibody that has been most commonly applied in similar studies.[18,34,35,39–42] We primarily focused on primary skin tumors with a total of 58 cases. To evaluate CD276 expression in primary skin tumors and lymph node metastases from the same patient, we also included 13 cases of paired primary tumors and lymph node metastases. In contrast to the prior report,[37] we found strong CD276 expression in both tumor cells and tumor vasculature (Figure 1C). Similarly, we observed strong CD276 expression at higher frequencies in tumor vasculature (81/84; 96.4%) compared to tumor cells (62/84; 73.8%) (Figure 1D). In 10 of 13 paired cases, we observed comparable CD276 expression in the tumor cells of both primary and metastatic tumors, indicating that CD276 expression was not correlated with metastatic disease in our study (Figure 1E). Due to insufficient cases, we were unable to evaluate CD276 expression in late-stage metastatic MCC tumors. Consistent with previous reports,[37] we did not observe higher CD276 expression levels in the tumor vasculature of lymph node metastatic tumors compared to primary skin tumors in all 13 paired cases. Thus, the frequently observed CD276 expression in this MCC patient tumor cohort highlights CD276 as a promising therapeutic target.

m276-SL-PBD attenuates MCC cell proliferation *in vitro*

There are currently two CD276-targeting ADCs under clinical evaluation, MGC018 (NCT05551117/NCT06227546) and DS-7300a (NCT05280470/NCT06330064), providing evidence of clinical feasibility. Compared to these, the CD276-ADC armed with pyrrolobenzodiazepine (m276-glyco-PBD) and the reengineered m276-SL-PBD which target both tumor cells and tumor vasculature have demonstrated the most potent anti-tumor activity with low recurrence rates in preclinical studies.[18,33,34] The modified m276-SL-PBD offers improved stability, target specificity, and enhanced potency without increased toxicity, while retaining the typical pharmacokinetic profile observed with the earlier m276-glyco-PBD.[33] To investigate m276-SL-PBD efficacy in MCC, we first tested its anti-proliferation activity against a panel of MCC cell lines (STAR Methods). In brief, MCC cells were exposed to serial concentrations of m276-SL-PBD (0–30 nM) for 72 h, and saline treated cells served as controls. Independent of MCPyV status, m276-SL-PBD exhibited potent inhibition of MCC cell proliferation largely consistent with CD276 expression levels (half maximal growth inhibitory concentration [GI_{50}] ranging from 2.3 nM to 19.6 nM) (Figure 2). m276-SL-PBD displayed high efficacy against MCC-9 and MKL-1 cell lines expressing high levels of CD276, with GI_{50} values of

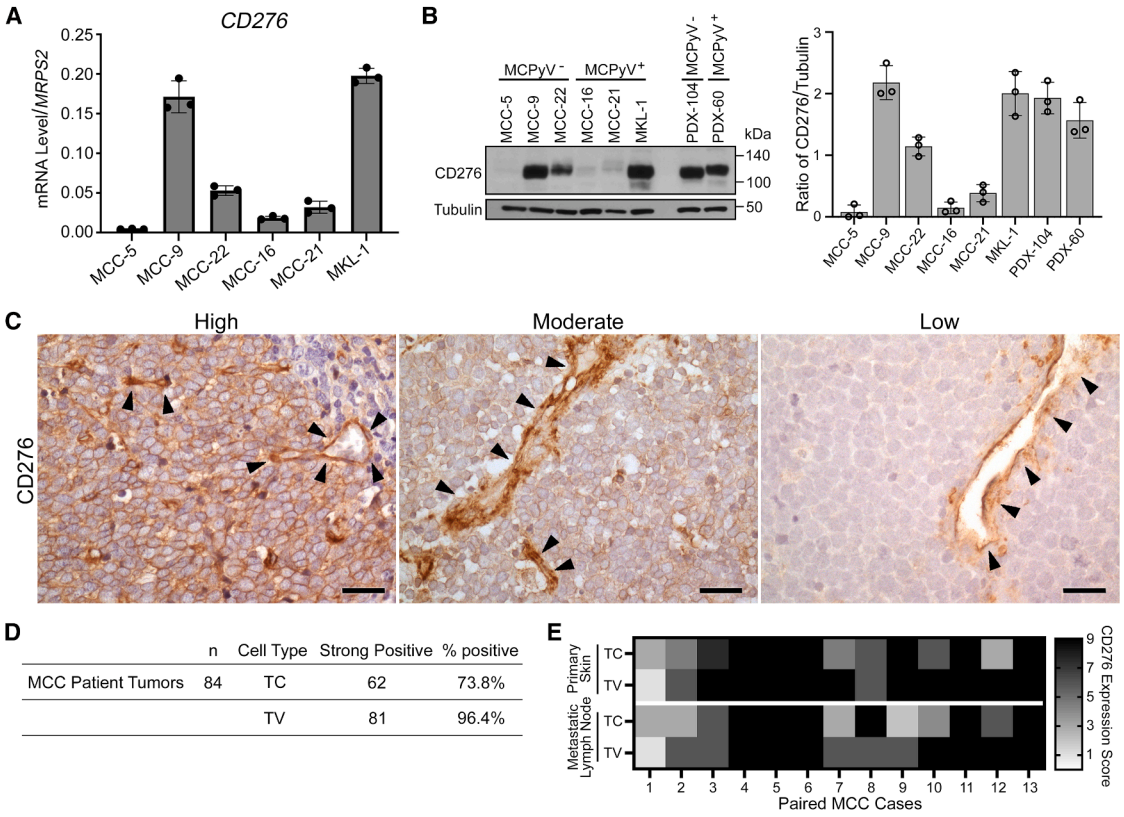

Figure 1. CD276 Expression in MCC cell lines, PDX tumors, and patient tumors

(A) Relative mRNA expression of *CD276* in six primary MCC cell lines normalized to *MRPS2* and presented as mean ± SD with samples run in triplicate.

(B) Immunoblot showing CD276 protein expression in six MCC cell lines and two PDX tumors (left). Ratios of CD276 to tubulin presented as mean ± SD (right).

(C) Representative MCC patient tumors with high, moderate, and low CD276 tumor cell membrane staining with strong CD276 expression in tumor-associated vasculature. Arrowheads indicate tumor vasculature. Scale bars, 70 μm.

(D) Table summarizing CD276 expression in 84 MCC patient tumors. TC: tumor cells and TV: tumor vasculature.

(E) Heatmap comparing CD276 expression in tumor cells and tumor vasculature in 13 paired primary skin tumors and local-regional lymph node metastases. See also Tables S1 and S2.

2.3 nM (95% confidence interval [CI] 1.4–3.7) and 2.7 nM (95% CI 1.3–5.4), respectively. MCC-21 and MCC-22 expressed moderate levels of CD276, with somewhat lower *in vitro* sensitivity to m276-SL-PBD with GI_{50} values of 15.5 nM (95% CI 12.7–18.8) and 19.6 nM (95% CI 15.6–25.0), respectively. As expected, MCC-5 and MCC-16 tumor cells with minimal CD276 expression were insensitive to m276-SL-PBD *in vitro* (data not shown).

m276-SL-PBD eradicates MCC cell line-derived xenografts in immunodeficient preclinical mouse models

Preclinical studies have shown that ADCs achieve greater antitumor effects when the targeted antigen is expressed in both tumor cells and tumor vasculature.[18,43] This dual targeting approach limits tumor growth and hinders metastatic dissemination, while also reducing the likelihood of developing drug resistance.[18,43,44] Significantly, m276-SL-PBD binds both human and mouse CD276 with similar affinity, allowing targeting of both human tumor cells and murine tumor vasculature, while monitoring off-target side effects in our preclinical mouse models.[18] To examine m276-SL-PBD efficacy, we generated cell line-derived xenograft (CDX) models in immunodeficient mice using MKL-1 cells (high CD276 expression), MCC-22 cells (moderate), and MCC-5 cells (minimal). With particular importance, our experimental design factored in variables such as tumor MCPyV status and mouse biological sex to evaluate potential impacts on treatment response. Of note, to examine m276-SL-PBD efficacy in well-established tumors, we used a higher average initial tumor volume threshold of $\geq$350 mm^3, rather than the typical $\geq$100 mm^3 upon randomization. Mice were maintained for 180 days post-randomization to monitor long-term response and potential relapse. Over the experimental course, mice were closely evaluated for health, and tumor measurements were taken three times weekly and presented as mean tumor volumes ± SEM. Complete response was achieved when the xenograft became undetectable or reduced to $\leq$50 mm^3 for at least two weeks.[45]

CDX models using MCPyV-positive MKL-1 cells and MCPyV-negative MCC-22 cells were generated in NOD *Rag* gamma mice (NRG) (Jackson Laboratory, strain #007799), as described

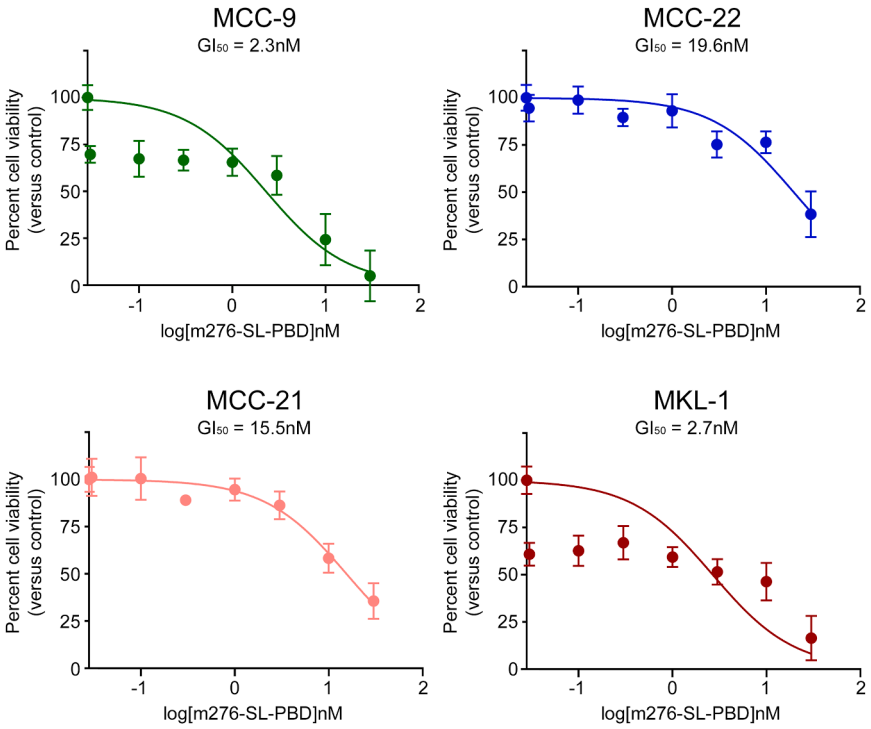

Figure 2. m276-SL-PBD inhibits MCC cell proliferation

MCC cell lines were exposed to serial concentrations of m276-SL-PBD (0–30 nM). Cell viability was assessed by colorimetric cell viability assay. The two data points plotted at the lowest concentration represent 0 nM (saline control) and 0.03 nM of m276-SL-PBD. Data presented as mean ± SEM, with half maximal growth inhibitory concentration (GI_{50}) analyzed by nonlinear regression model using GraphPad Prism.

previously.[1] When xenografts reached an average volume of 350 mm^3, CDX MKL-1 mice were randomized into control (n = 5) and treatment (n = 13) groups followed by four weekly doses of vehicle or m276-SL-PBD (0.5 mg/kg), respectively (Figure 3A). By day 13 post-randomization, the control group rapidly reached tumor growth endpoint and was humanely euthanized. Meanwhile, m276-SL-PBD treatment repressed tumor growth and resulted in a complete response as early as day 29, with the last mouse showing no measurable tumor on day 55. All mice in the treatment group (13/13) achieved complete response, with nearly 70% (9/13) remaining continuously tumor-free through day 180 (experimental endpoint) (Figure 3B). Four mice began showing signs of relapse starting on day 72 (after maintaining complete response for nearly a month) and were retreated when relapsed tumors reached retreatment threshold of ∼500 mm^3 (Figure 3A). Three relapsed tumors demonstrated significant regression upon retreatment, and two retreated mice were sacrificed to evaluate CD276 expression in response to treatment. The fourth mouse did not receive m276-SL-PBD because its tumor remained below the retreatment threshold (500 mm^3) by the experimental endpoint (as indicated by * in Figure 3A), and tissue was collected for examination of CD276 expression. We found that CD276 expression remained high in relapsed tumor and decreased in response to treatment (Figure 3C), indicating m276-SL-PBD maintains potency and circumvents potential resistance in relapsed xenografts with CD276 expression.

Previous studies have established the target specificity of m276-glyco-PBD, demonstrating that both the parent monoclonal antibody (mAb) and the payload alone exhibit minimal anti-tumor activity *in vivo*,[18] and isotype controls employing nonspecific isotype conjugated to PBD (IgG-SL-PBD) have shown negligible effects on anti-tumor activities *in vitro*.[33] To confirm if this is the case in our study, IgG-SL-PBD was tested in the MKL-1 CDX model. Tumor-bearing mice were assigned to groups receiving four weekly doses of either saline (n = 5) or IgG-SL-PBD (n = 5; 0.5 mg/kg). Compared to saline treatment, IgG-SL-PBD initially slowed tumor growth but xenografts rebounded and reached tumor volume endpoint on day 82–91 (Figure S3). Importantly, IgG-SL-PBD failed to provide any survival benefit, highlighting that specifically targeting CD276 was crucial for achieving long-term remission. Due to this lack of survival benefit and the high cost of manufacturing IgG-SL-PBD, we utilized saline controls for *in vivo* studies.

To evaluate whether biological sex of the mouse model impacts treatment response, we tested m276-SL-PBD in both male and female NRG mice using the MCC-22 primary cell line. Tumor-bearing mice were randomized and treated with either m276-SL-PBD or vehicle following the same regimen as specified earlier (Figures 3D and 3E). Male and female mice in the control groups (n = 8 for each respective control) reached tumor endpoint at day 17 and day 22 post-randomization, respectively. Complete tumor regression was observed in all male mice receiving m276-SL-PBD (n = 8) between day 35–65 and in all female mice (n = 8) between day 39–65. A single male mouse in the treatment group was found dead on day 139, with no evidence of tumor relapse. Within the treatment groups, all female mice and the remaining seven male mice demonstrated tumor-free survival until experimental endpoint (day 180 post-randomization) (Figure 3F). Taken together, these findings demonstrate that m276-SL-PBD exhibits potent anti-tumor efficacy in MCC CDX models, independent of MCPyV status, with similarly robust efficacy in both male and female mice.

To determine if m276-SL-PBD is effective in MCC tumors with low CD276 expression, we generated a CDX mouse model using MCC-5 cells with minimal CD276 expression among six MCC cell lines examined. When MCC-5 xenografts reached 350 mm^3, mice were assigned to receive either vehicle (n = 5) or m276-SL-PBD (n = 10). Mice received five weekly doses of m276-SL-PBD (0.5 mg/kg) to account for the minimal CD276 target site availability in MCC-5 tumor cells. Control mice

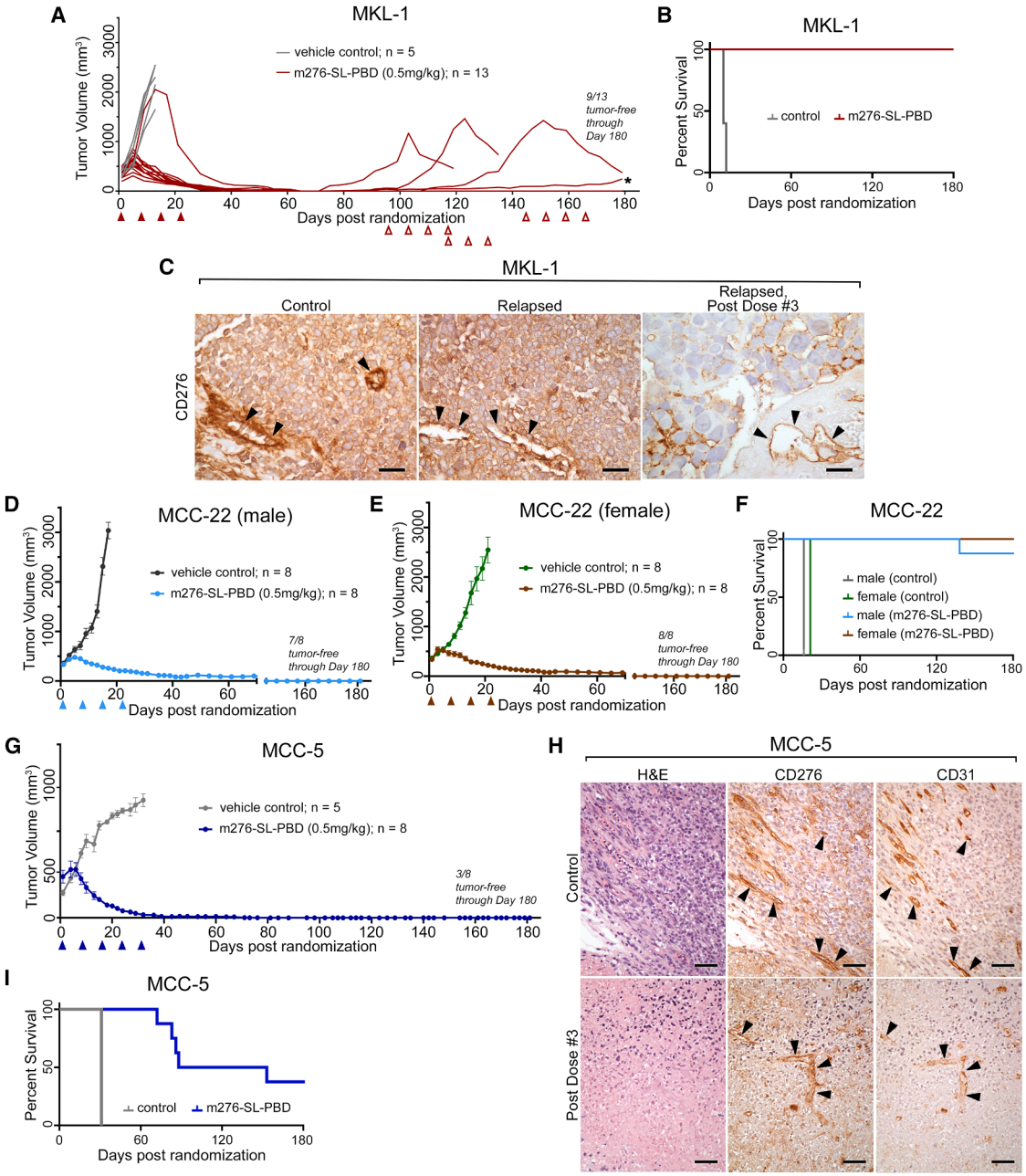

Figure 3. m276-SL-PBD induces long-term survival in MCC CDX mouse models

All tumor volumes presented as mean volume ± SEM, with treatment days indicated by solid arrowheads.

(A) MKL-1 CDX growth in mice receiving vehicle control or m276-SL-PBD, with solid lines representing individual mice. Three relapsed tumors were retreated as indicated by open red arrowheads, and one relapsed tumor (which did not reach retreatment threshold) is indicated by asterisk.

(B) Kaplan-Meier survival analysis of MKL-1 CDX mice.

(C) Representative CD276 staining in MKL-1 xenografts from a mouse receiving vehicle control (left), a mouse with relapsed tumor (middle), and a mouse with relapsed tumor euthanized after the third retreatment dose of m276-SL-PBD (right). Arrowheads indicate tumor vasculature. Scale bars, 70 μm.

(D and E) MCC-22 xenograft growth in (D) male mice and (E) female mice receiving vehicle control or m276-SL-PBD.

(F) Kaplan-Meier survival analysis of male and female MCC-22 CDX mice.

(G) MCC-5 CDX growth receiving vehicle control or m276-SL-PBD.

(H) Representative H&E, CD276, and CD31 staining in consecutive sections of MCC-5 xenografts from a mouse receiving vehicle control (top panel) and a mouse euthanized after the third dose of m276-SL-PBD (bottom panel). Arrowheads indicate tumor vasculature. Scale bars, 35 μm. See Figure S4 for higher magnification images.

(I) Kaplan-Meier survival analysis of MCC-5 CDX models.

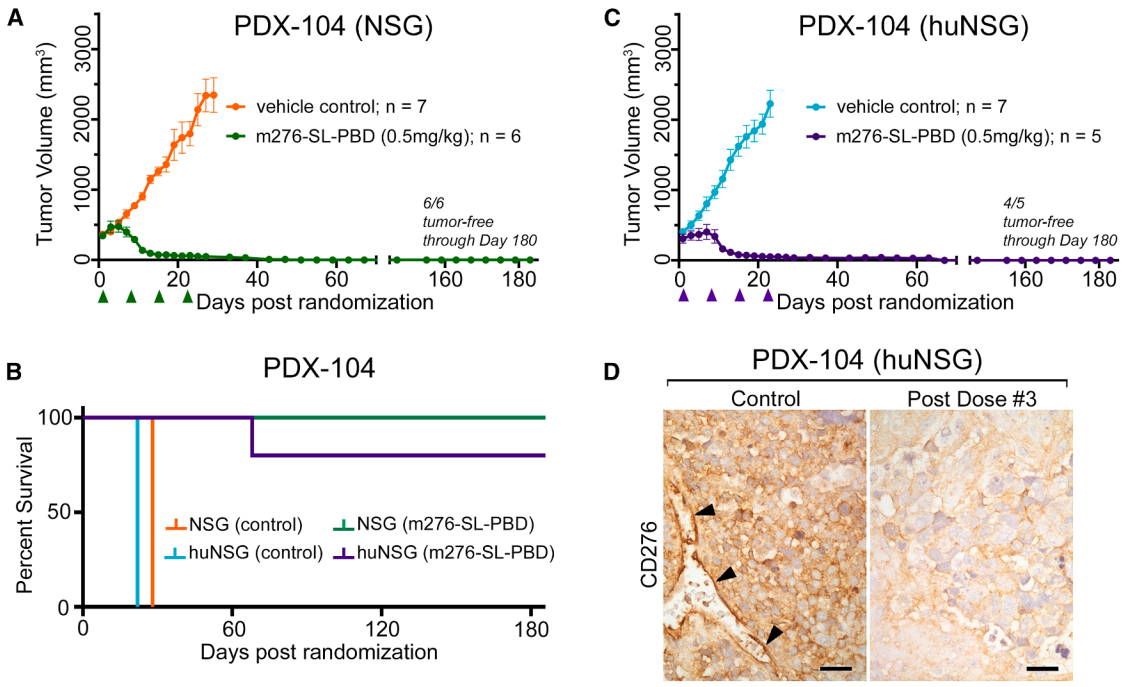

Figure 4. m276-SL-PBD induces long-term survival in immunodeficient and immuno-competent MCC PDX models

All tumor volumes presented as mean volume ± SEM, with treatment days indicated by solid arrowheads.

(A and C) PDX-104 xenograft growth in (A) NSG mice and (C) huNSG mice receiving control or m276-SL-PBD (0.5 mg/kg) as indicated by arrowheads. Tumor volume presented as mean ± SEM.

(B) Kaplan Meier survival analysis of NSG and huNSG PDX-104 models.

(D) Representative CD276 staining in PDX-104 huNSG xenografts from a mouse receiving vehicle control (left) and a mouse euthanized after the third dose of m276-SL-PBD (right). Arrowheads indicate tumor vasculature. Scale bars, 70 μm.

reached tumor growth endpoint by day 32. Two treatment mice were sacrificed after the second and third doses for evaluation of CD276 expression and excluded from long-term survival analysis. Remarkably, complete resolution of xenografts was observed in three of eight remaining m276-SL-PBD-treated mice by day 43, another four mice by day 73, and the last mouse by day 105 (Figure 3G). While minimal CD276 expression was detected in MCC-5 cells (Figure S4), high CD276 expression was observed in CD31^{+} murine endothelial cells in xenografts from both control and treatment groups. However, the number of CD276-expressing tumor vessels was significantly decreased in response to treatment (Figure 3H). Notably, m276-SL-PBD binds both human and mouse CD276 with similar affinity, and the observed effects in MCC-5 xenografts might be attributed to m276-SL-PBD targeting murine endothelial cells. This is supported by the extensive areas of necrotic tumor cells observed in the treated xenograft tumor, suggesting that targeting tumor vasculature alone is effective in MCC (Figures 3H and S4). Additionally, the observed widespread tumor cell death may be due to potential bystander effects of free PBD within the TME, as previously reported.[18,46,47] Notably, three of eight mice treated with m276-SL-PBD survived with no measurable tumor through the experimental endpoint (day 180 post-randomization). Five treated mice reached humane endpoints between day 73 and 154 (Figure 3I). As these events occurred well beyond its half-life of 81 h,[33] the observed poor health was unlikely related to m276-SL-PBD treatment. Histological examination of livers from these mice revealed no obvious signs of toxicity (Figure S2). Thus, the ability of m276-SL-PBD to completely eradicate all MCC-5 xenografts and significantly prolong survival for up to 6 months underscores targeting CD276-expressing vasculature as a key component of its potency.

m276-SL-PBD eradicates MCC PDXs in immunodeficient and immune-competent preclinical mouse models

Given that PDX models are considered the most biologically relevant preclinical platform due to their preservation of primary tumor heterogeneity, we further evaluated the therapeutic potential of m276-SL-PBD with our PDX-104 model in immunodeficient NOD *scid* gamma (NSG) mice (Jackson Laboratory, strain #005557), which were chosen in order to be consistent with the CD34^{+} humanized NSG mice used in the study described in the following text. PDX-104 NSG mice were randomized into control (n = 7) and treatment (n = 6) groups following the same treatment regimen described earlier (Figure 4A). The control group reached tumor endpoint at day 29 post-randomization. Strikingly, m276-SL-PBD induced complete tumor eradication in four mice before the administration of the fourth weekly dose on day 22 and in the remaining two mice on days 31 and 51. All PDX-104 NSG mice receiving m276-SL-PBD showed tumor-free survival until experimental endpoint at 180 days post-randomization (Figure 4B).

While immunodeficient mice have served as valuable tools in preclinical drug efficacy studies,[45,48] these models do not recapitulate the TME in humans, which is especially important to consider when targeting CD276, an immunoregulatory ligand known to play a role in T cell regulation.[27,32] Recently, "humanized" mice (huNSG) with intact immune systems generated by engraftment of human $CD34^+$ hematopoietic stem cells (only available in female immunodeficient NSG mice) have served as a powerful tool for immuno-oncology studies.[48] To leverage the more clinically relevant PDX model in a preclinical setting mimicking the patient TME, we evaluated m276-SL-PBD in huNSG PDX-104 xenografts, which were randomized into control ($n = 7$) and treatment ($n = 7$) groups following the same treatment regimen as specified earlier (Figure 4C). The control group reached tumor endpoint at day 23 post-randomization. Of the seven mice in the treatment cohort, two mice were sacrificed after the third dose for evaluation of CD276 expression, and were thus excluded from the long-term survival analysis. In the remaining five treatment group mice, m276-SL-PBD completely suppressed tumor growth in three mice by the third dose on day 15 and in one mouse by day 67; all four of these mice demonstrated extended tumor-free survival through day 180 (Figure 4B). The fifth mouse showed complete tumor eradication on day 29 and maintained complete response for almost six weeks, but was found dead on day 69 with no obvious cause and no evidence of relapse. We observed a dramatic reduction in the number of CD276-expressing tumor cells in the treated xenografts compared to controls, suggesting that m276-SL-PBD specifically ablated tumor cells with CD276 expression (Figure 4D). We found similar abundance of human $CD45^+$, $CD3^+$, and $CD4^+$ immune cells in treatment and control PDX-104 huNSG xenografts, indicating that m276-SL-PBD maintained its potency with no adverse effect on immune cells (Figure S5).

Importantly, through the 180-day experimental course, m276-SL-PBD was well tolerated with no significant changes in body weight (Figure S1), activity, and food/water intake. Moreover, histological evaluation of liver specimens collected from treated mice across each animal model revealed no evidence of liver toxicity when compared to the control groups (Figure S2).

DISCUSSION

In this study, we have shown that CD276 is often highly expressed in MCC patient tumor cells and tumor vasculature, supporting its potential as an effective therapeutic target in MCC. We have further provided compelling evidence of m276-SL-PBD as a highly potent therapy in multiple MCC CDX and PDX models. Notably, m276-SL-PBD treatment resulted in complete elimination of xenografts in all mice (48/48), with durable tumor-free response observed in 82% of mice through the 180-day experimental course, independent of MCPyV status. Of note, there were no notable adverse effects observed across all tested models. Critically, m276-SL-PBD evaded potential drug resistance and retained efficacy in relapsed tumors with sustained CD276 expression, underscoring its potential clinical application. With high clinical relevance, we have first established humanized $CD34^+$ MCC PDX models with intact human immune systems and demonstrated long-lasting treatment effect of m276-SL-PBD in a preclinical platform that most closely resembles the patient TME, with no obvious activity against human immune cells. Taken together, these results imply great potential for bench-to-bedside translation.

Consistent with prior findings,[37] CD276 expression was detected in a high percentage of tumor vasculature in MCC patient tumors (96.4%). Of note, we also revealed CD276 expression in MCC patient tumor cells, with our findings further validated at the protein and transcript levels in primary MCC cell lines and PDXs. It is unclear why this differs from the published finding,[37] however, we employed a different anti-CD276 antibody, which has been widely used and validated in similar studies.[18,34,35,39–42] In contrast to other studies suggesting that CD276 expression is higher in metastatic tumors,[28,30,31] we and Aung et al.[37] did not observe increased CD276 expression in metastatic tumors compared to paired primary tumors. Future studies are required to delineate CD276 expression in primary and distant MCC metastases and its correlation with patient survival.

ADCs are an emergent field in cancer therapy, allowing precise localization of cytotoxic agents to tumor cells expressing specific antigens and offering certain advantages over "naked" antibody or traditional chemotherapy.[17,19,49] In MCC preclinical studies, the CD56-targeting ADC Adcitmer showed limited efficacy, only delaying tumor growth without achieving complete responses.[22] In contrast, m276-SL-PBD eradicated xenografts with long-lasting treatment response. Moreover, MGC018 and DS-7300a, both CD276-targeting ADCs advancing in clinical trials, have shown tumor-eradicating effects in preclinical studies across a range of human cancers.[35,36] However, these studies predominantly initiate treatment at earlier tumor stages, mostly around 150 mm^3, with observation periods concluding within 30–50 days after treatment start. With high clinical relevance, our work with m276-SL-PBD addresses conditions characteristic of advanced disease by initiating treatment at an average volume $\geq$350 mm^3, while still achieving complete tumor eradication with tumor-free survival extending up to 180 days after treatment start. This approach provides a rigorous evaluation of m276-SL-PBD's potency and durability against locally advanced tumors.

It has been shown that antigen expression in both tumor cells and tumor vasculature improves the overall efficacy of ADCs.[18,43,50] Tumor vasculature serves as a more mutation-resistant target than tumor cells, likely enhancing the durability of response and potentially reducing the likelihood of drug resistance. Our MCC-5 CDX model suggests that targeting CD276-expressing tumor vasculature is effective regardless of CD276 expression in MCC tumor cells. Though recent findings suggest that *in vitro* assays predict m276-SL-PBD sensitivity,[33] our findings suggest that therapeutic efficacy is also driven by its effects within the TME, which is not captured by *in vitro* assays. Thus, detection of CD276 in patient tumors and TME could offer a more comprehensive and accurate means of patient stratification.

In summary, our study has provided compelling evidence for CD276 as a promising therapeutic target, and for m276-SL-PBD as a potent and effective therapy for patients suffering

from MCC, other neuroendocrine carcinomas, or human cancers with neuroendocrine transformation, and justifies future clinical investigation.

Limitations of the study

We acknowledge that there are several limitations in the current study. First, while we demonstrate the potent preclinical efficacy of m276-SL-PBD in multiple MCC models, clinical studies are needed to evaluate its safety, pharmacokinetics, and therapeutic potential in human patients. Furthermore, though the long-term survival benefit from m276-SL-PBD treatment clearly validates CD276 as a therapeutic target, the delayed tumor growth observed in IgG-SL-PBD-treated mice suggests potential non-specific effects due to the highly cytotoxic warhead (PBD), such as payload release, bystander effects, or non-specific uptake. Further mechanistic studies evaluating m276-SL-PBD stability, tissue distribution, and free payload levels in circulation would provide valuable insights regarding its specificity. Finally, it would be interesting to determine m276-SL-PBD efficacy in preclinical models of spontaneous metastases.

RESOURCE AVAILABILITY

Lead contact

Further information and resource requests should be directed to and will be fulfilled by the lead contact, Dr. Ling Gao (ling.gao@va.gov).

Materials availability

This study did not generate unique materials.

Data and code availability

- Data: This paper does not report or utilize original datasets.
- Code: This paper does not report original code.
- Other items: No other original resources.

ACKNOWLEDGMENTS

This work was funded by Merit Review Award (#I01CX002497) from the United States Department of Veterans Affairs through the Clinical Sciences Research and Development Service and by the National Institutes of Health, through the National Cancer Institute under award number R01CA266514-01, as well as resources and use of facilities at the VA Long Beach Healthcare System. We extend our deepest gratitude to the Southern California Institute for Research and Education, Cooperative Human Tissue Network (CHTN), UC-Irvine Department of Dermatology, and Mitchell and Joan Markow of the Two Sisters Foundation. We also wish to acknowledge the support of the Chao Family Comprehensive Cancer Center's Experimental Tissue Resource, a Shared Resource supported by the National Cancer Institute of the National Institutes of Health under award number P30CA062203.

The content is solely the responsibility of the authors and does not necessarily represent the official views of the National Institutes of Health, the Department of Veterans Affairs, or the United States Government.

AUTHOR CONTRIBUTIONS

Conceptualization, M.D.K, H.Z., and L.G.; methodology, M.D.K., A.K., G.J.V., Y.F., S.S., B.K.D., D.P., N.L., H.Z., B.S.C., and L.G.; investigation, M.D.K., A. K., G.J.V., Y.F., S.S., B.K.D., D.P., N.L., H.Z., B.S.C., and L.G.; visualization, M.D.K., A.K., B.K.D., H.Z., and L.G.; funding acquisition, L.G.; project administration, H.Z. and L.G.; supervision, L.G.; writing – original draft, M.D.K., A.K., H.Z., and L.G.; writing – review and editing: M.D.K., A.K., B.K.D., H.Z., and L.G.

DECLARATION OF INTERESTS

S.S. and B.S.C. are inventors of intellectual property related to CD276 antibodies and ADCs, and B.S.C. has received research support through a Cooperative Research and Development Agreement between BioMed Valley Discoveries and the National Cancer Institute.

STAR★METHODS

Detailed methods are provided in the online version of this paper and include the following:

- KEY RESOURCES TABLE
- EXPERIMENTAL MODEL AND SUBJECT DETAILS
  - Patient samples
  - Cell lines
  - Animal participants
- METHOD DETAILS
  - Cell culture
  - Quantitative real-time PCR
  - Immunoblot analysis
  - Immunohistochemistry
  - Cell viability and proliferation assay
  - Generation of MCC patient-derived xenograft (PDX) lineage
  - m276-SL-PBD preclinical drug studies
- QUANTIFICATION AND STATISTICAL ANALYSIS

SUPPLEMENTAL INFORMATION

Supplemental information can be found online at https://doi.org/10.1016/j.isci.2025.112436.

Received: June 7, 2023
Revised: December 30, 2024
Accepted: April 10, 2025
Published: April 15, 2025

REFERENCES

1. Fang, B., Kannan, A., Zhao, S., Nguyen, Q.H., Ejadi, S., Yamamoto, M., Camilo Barreto, J., Zhao, H., and Gao, L. (2020). Inhibition of PI3K by copanlisib exerts potent antitumor effects on Merkel cell carcinoma cell lines and mouse xenografts. Sci. Rep. *10*, 8867. https://doi.org/10.1038/s41598-020-65637-2.
2. Fitzgerald, T.L., Dennis, S., Kachare, S.D., Vohra, N.A., Wong, J.H., and Zervos, E.E. (2015). Dramatic Increase in the Incidence and Mortality from Merkel Cell Carcinoma in the United States. Am. Surg. *81*, 802–806. https://doi.org/10.1177/000313481508100819.
3. Harms, K.L., Healy, M.A., Nghiem, P., Sober, A.J., Johnson, T.M., Bichakjian, C.K., and Wong, S.L. (2016). Analysis of Prognostic Factors from 9387 Merkel Cell Carcinoma Cases Forms the Basis for the New 8th Edition AJCC Staging System. Ann. Surg Oncol. *23*, 3564–3571. https://doi.org/10.1245/s10434-016-5266-4.
4. Lebbe, C., Becker, J.C., Grob, J.J., Malvehy, J., Del Marmol, V., Pehamberger, H., Peris, K., Saiag, P., Middleton, M.R., Bastholt, L., et al. (2015). Diagnosis and treatment of Merkel Cell Carcinoma. European consensus-based interdisciplinary guideline. Eur. J. Cancer *51*, 2396–2403. https://doi.org/10.1016/j.ejca.2015.06.131.
5. Paulson, K.G., Park, S.Y., Vandeven, N.A., Lachance, K., Thomas, H., Chapuis, A.G., Harms, K.L., Thompson, J.A., Bhatia, S., Stang, A., and Nghiem, P. (2018). Merkel cell carcinoma: Current US incidence and projected increases based on changing demographics. J. Am. Acad. Dermatol. *78*, 457–463.e2. https://doi.org/10.1016/j.jaad.2017.10.028.
6. Colunga, A., Pulliam, T., and Nghiem, P. (2018). Merkel Cell Carcinoma in the Age of Immunotherapy: Facts and Hopes. Clin. Cancer Res. *24*, 2035–2043. https://doi.org/10.1158/1078-0432.Ccr-17-0439.

7. Feng, H., Shuda, M., Chang, Y., and Moore, P.S. (2008). Clonal integration of a polyomavirus in human Merkel cell carcinoma. Science *319*, 1096–1100. https://doi.org/10.1126/science.1152586.

8. Santos-Juanes, J., Fernández-Vega, I., Fuentes, N., Galache, C., Coto-Segura, P., Vivanco, B., Astudillo, A., and Martínez-Camblor, P. (2015). Merkel cell carcinoma and Merkel cell polyomavirus: a systematic review and meta-analysis. Br. J. Dermatol. *173*, 42–49. https://doi.org/10.1111/bjd.13870.

9. Knepper, T.C., Montesion, M., Russell, J.S., Sokol, E.S., Frampton, G.M., Miller, V.A., Albacker, L.A., McLeod, H.L., Eroglu, Z., Khushalani, N.I., et al. (2019). The Genomic Landscape of Merkel Cell Carcinoma and Clinicogenomic Biomarkers of Response to Immune Checkpoint Inhibitor Therapy. Clin. Cancer Res. *25*, 5961–5971. https://doi.org/10.1158/1078-0432.Ccr-18-4159.

10. D'Angelo, S.P., Russell, J., Lebbé, C., Chmielowski, B., Gambichler, T., Grob, J.J., Kiecker, F., Rabinowits, G., Terheyden, P., Zwiener, I., et al. (2018). Efficacy and Safety of First-line Avelumab Treatment in Patients With Stage IV Metastatic Merkel Cell Carcinoma: A Preplanned Interim Analysis of a Clinical Trial. JAMA Oncol. *4*, e180077. https://doi.org/10.1001/jamaoncol.2018.0077.

11. Gallo, M., Guarnotta, V., De Cicco, F., Rubino, M., Faggiano, A., and Colao, A.; NIKE Group (2019). Immune checkpoint blockade for Merkel cell carcinoma: actual findings and unanswered questions. J. Cancer Res. Clin. Oncol. *145*, 429–443. https://doi.org/10.1007/s00432-019-02839-w.

12. Harms, P.W., Harms, K.L., Moore, P.S., DeCaprio, J.A., Nghiem, P., Wong, M.K.K., and Brownell, I.; International Workshop on Merkel Cell Carcinoma Research IWMCC Working Group (2018). The biology and treatment of Merkel cell carcinoma: current understanding and research priorities. Nat. Rev. Clin. Oncol. *15*, 763–776. https://doi.org/10.1038/s41571-018-0103-2.

13. Kaufman, H.L., Russell, J., Hamid, O., Bhatia, S., Terheyden, P., D'Angelo, S.P., Shih, K.C., Lebbé, C., Linette, G.P., Milella, M., et al. (2016). Avelumab in patients with chemotherapy-refractory metastatic Merkel cell carcinoma: a multicentre, single-group, open-label, phase 2 trial. Lancet Oncol. *17*, 1374–1385. https://doi.org/10.1016/s1470-2045(16)30364-3.

14. Nghiem, P.T., Bhatia, S., Lipson, E.J., Kudchadkar, R.R., Miller, N.J., Annamalai, L., Berry, S., Chartash, E.K., Daud, A., Fling, S.P., et al. (2016). PD-1 Blockade with Pembrolizumab in Advanced Merkel-Cell Carcinoma. N. Engl. J. Med. *374*, 2542–2552. https://doi.org/10.1056/NEJMoa1603702.

15. Rastrelli, M., Del Fiore, P., Russo, I., Tartaglia, J., Dal Monico, A., Cappellesso, R., Nicolè, L., Piccin, L., Fabozzi, A., Biffoli, B., et al. (2021). Merkel Cell Carcinoma: Evaluation of the Clinico-Pathological Characteristics, Treatment Strategies and Prognostic Factors in a Monocentric Retrospective Series (n=143). Front. Oncol. *11*, 737842. https://doi.org/10.3389/fonc.2021.737842.

16. Chau, C.H., Steeg, P.S., and Figg, W.D. (2019). Antibody-drug conjugates for cancer. Lancet *394*, 793–804. https://doi.org/10.1016/s0140-6736(19)31774-x.

17. Esnault, C., Schrama, D., Houben, R., Guyétant, S., Desgranges, A., Martin, C., Berthon, P., Viaud-Massuard, M.C., Touzé, A., Kervarrec, T., and Samimi, M. (2022). Antibody-Drug Conjugates as an Emerging Therapy in Oncodermatology. Cancers (Basel) *14*, 778. https://doi.org/10.3390/cancers14030778.

18. Seaman, S., Zhu, Z., Saha, S., Zhang, X.M., Yang, M.Y., Hilton, M.B., Morris, K., Szot, C., Morris, H., Swing, D.A., et al. (2017). Eradication of Tumors through Simultaneous Ablation of CD276/B7-H3-Positive Tumor Cells and Tumor Vasculature. Cancer Cell *31*, 501–515.e8. https://doi.org/10.1016/j.ccell.2017.03.005.

19. Tong, J.T.W., Harris, P.W.R., Brimble, M.A., and Kavianinia, I. (2021). An Insight into FDA Approved Antibody-Drug Conjugates for Cancer Therapy. Molecules *26*, 5847. https://doi.org/10.3390/molecules26195847.

20. Liu, K., Li, M., Li, Y., Li, Y., Chen, Z., Tang, Y., Yang, M., Deng, G., and Liu, H. (2024). A review of the clinical efficacy of FDA-approved antibody–drug conjugates in human cancers. Mol. Cancer *23*, 62. https://doi.org/10.1186/s12943-024-01963-7.

21. Zeromski, J., Nyczak, E., and Dyszkiewicz, W. (2001). Significance of cell adhesion molecules, CD56/NCAM in particular, in human tumor growth and spreading. Folia Histochem. Cytobiol. *39*, 36–37.

22. Esnault, C., Leblond, V., Martin, C., Desgranges, A., Baltus, C.B., Aubrey, N., Lakhrif, Z., Lajoie, L., Lantier, L., Clémenceau, B., et al. (2022). Adcitmer(®) , a new CD56-targeting monomethyl auristatin E-conjugated antibody, is a potential therapeutic approach in Merkel cell carcinoma. Br. J. Dermatol. *186*, 295–306. https://doi.org/10.1111/bjd.20770.

23. Ollier, J., Kervarrec, T., Samimi, M., Benlalam, H., Aumont, P., Vivien, R., Touzé, A., Labarrière, N., Vié, H., and Clémenceau, B. (2018). Merkel cell carcinoma and cellular cytotoxicity: sensitivity to cellular lysis and screening for potential target antigens suitable for antibody-dependent cellular cytotoxicity. Cancer Immunol. Immunother. *67*, 1209–1219. https://doi.org/10.1007/s00262-018-2176-2.

24. Shah, M.H., Lorigan, P., O'Brien, M.E.R., Fossella, F.V., Moore, K.N., Bhatia, S., Kirby, M., and Woll, P.J. (2016). Phase I study of IMGN901, a CD56-targeting antibody-drug conjugate, in patients with CD56-positive solid tumors. Invest. New Drugs *34*, 290–299. https://doi.org/10.1007/s10637-016-0336-9.

25. Tetzlaff, M.T., and Harms, P.W. (2020). Danger is only skin deep: aggressive epidermal carcinomas. An overview of the diagnosis, demographics, molecular-genetics, staging, prognostic biomarkers, and therapeutic advances in Merkel cell carcinoma. Mod. Pathol. *33*, 42–55. https://doi.org/10.1038/s41379-019-0394-6.

26. Socinski, M.A., Kaye, F.J., Spigel, D.R., Kudrik, F.J., Ponce, S., Ellis, P.M., Majem, M., Lorigan, P., Gandhi, L., Gutierrez, M.E., et al. (2017). Phase 1/2 Study of the CD56-Targeting Antibody-Drug Conjugate Lorvotuzumab Mertansine (IMGN901) in Combination With Carboplatin/Etoposide in Small-Cell Lung Cancer Patients With Extensive-Stage Disease. Clin. Lung Cancer *18*, 68–76.e2. https://doi.org/10.1016/j.cllc.2016.09.002.

27. Collins, M., Ling, V., and Carreno, B.M. (2005). The B7 family of immune-regulatory ligands. Genome Biol. *6*, 223. https://doi.org/10.1186/gb-2005-6-6-223.

28. Getu, A.A., Tigabu, A., Zhou, M., Lu, J., Fodstad, Ø., and Tan, M. (2023). New frontiers in immune checkpoint B7-H3 (CD276) research and drug development. Mol. Cancer *22*, 43. https://doi.org/10.1186/s12943-023-01751-9.

29. Zhao, B., Li, H., Xia, Y., Wang, Y., Wang, Y., Shi, Y., Xing, H., Qu, T., Wang, Y., and Ma, W. (2022). Immune checkpoint of B7-H3 in cancer: from immunology to clinical immunotherapy. J. Hematol. Oncol. *15*, 153. https://doi.org/10.1186/s13045-022-01364-7.

30. Zhou, W.T., and Jin, W.L. (2021). B7-H3/CD276: An Emerging Cancer Immunotherapy. Front. Immunol. *12*, 701006. https://doi.org/10.3389/fimmu.2021.701006.

31. Picarda, E., Ohaegbulam, K.C., and Zang, X. (2016). Molecular Pathways: Targeting B7-H3 (CD276) for Human Cancer Immunotherapy. Clin. Cancer Res. *22*, 3425–3431. https://doi.org/10.1158/1078-0432.Ccr-15-2428.

32. Kontos, F., Michelakos, T., Kurokawa, T., Sadagopan, A., Schwab, J.H., Ferrone, C.R., and Ferrone, S. (2021). B7-H3: An Attractive Target for Antibody-based Immunotherapy. Clin. Cancer Res. *27*, 1227–1235. https://doi.org/10.1158/1078-0432.Ccr-20-2584.

33. Feng, Y., Lee, J., Yang, L., Hilton, M.B., Morris, K., Seaman, S., Edupuganti, V.V.S.R., Hsu, K.S., Dower, C., Yu, G., et al. (2023). Engineering CD276/B7-H3-targeted antibody-drug conjugates with enhanced cancer-eradicating capability. Cell Rep. *42*, 113503. https://doi.org/10.1016/j.celrep.2023.113503.

34. Kendsersky, N.M., Lindsay, J., Kolb, E.A., Smith, M.A., Teicher, B.A., Erickson, S.W., Earley, E.J., Mosse, Y.P., Martinez, D., Pogoriler, J., et al. (2021). The B7-H3-Targeting Antibody-Drug Conjugate m276-SL-PBD Is Potently Effective Against Pediatric Cancer Preclinical Solid Tumor Models. Clin. Cancer Res. *27*, 2938–2946. https://doi.org/10.1158/1078-0432.Ccr-20-4221.

35. Scribner, J.A., Brown, J.G., Son, T., Chiechi, M., Li, P., Sharma, S., Li, H., De Costa, A., Li, Y., Chen, Y., et al. (2020). Preclinical Development of MGC018, a Duocarmycin-based Antibody-drug Conjugate Targeting B7-H3 for Solid Cancer. Mol. Cancer Ther. *19*, 2235–2244. https://doi.org/10.1158/1535-7163.Mct-20-0116.

36. Yamato, M., Hasegawa, J., Maejima, T., Hattori, C., Kumagai, K., Watanabe, A., Nishiya, Y., Shibutani, T., Aida, T., Hayakawa, I., et al. (2022). DS-7300a, a DNA Topoisomerase I Inhibitor, DXd-Based Antibody-Drug Conjugate Targeting B7-H3, Exerts Potent Antitumor Activities in Preclinical Models. Mol. Cancer Ther. *21*, 635–646. https://doi.org/10.1158/1535-7163.Mct-21-0554.

37. Aung, P.P., Parra, E.R., Barua, S., Sui, D., Ning, J., Mino, B., Ledesma, D. A., Curry, J.L., Nagarajan, P., Torres-Cabala, C.A., et al. (2019). B7-H3 Expression in Merkel Cell Carcinoma-Associated Endothelial Cells Correlates with Locally Aggressive Primary Tumor Features and Increased Vascular Density. Clin. Cancer Res. *25*, 3455–3467. https://doi.org/10.1158/1078-0432.Ccr-18-2355.

38. Dong, P., Xiong, Y., Yue, J., Hanley, S.J.B., and Watari, H. (2018). B7H3 As a Promoter of Metastasis and Promising Therapeutic Target. Front. Oncol. *8*, 264. https://doi.org/10.3389/fonc.2018.00264.

39. Crispen, P.L., Sheinin, Y., Roth, T.J., Lohse, C.M., Kuntz, S.M., Frigola, X., Thompson, R.H., Boorjian, S.A., Dong, H., Leibovich, B.C., et al. (2008). Tumor cell and tumor vasculature expression of B7-H3 predict survival in clear cell renal cell carcinoma. Clin. Cancer Res. *14*, 5150–5157. https://doi.org/10.1158/1078-0432.Ccr-08-0536.

40. Ganesan, B., Parameswaran, S., Sharma, A., and Krishnakumar, S. (2020). Clinical relevance of B7H3 expression in retinoblastoma. Sci. Rep. *10*, 10185. https://doi.org/10.1038/s41598-020-67101-7.

41. Zang, X., Sullivan, P.S., Soslow, R.A., Waitz, R., Reuter, V.E., Wilton, A., Thaler, H.T., Arul, M., Slovin, S.F., Wei, J., et al. (2010). Tumor associated endothelial expression of B7-H3 predicts survival in ovarian carcinomas. Mod. Pathol. *23*, 1104–1112. https://doi.org/10.1038/modpathol.2010.95.

42. Zhan, S., Liu, Z., Zhang, M., Guo, T., Quan, Q., Huang, L., Guo, L., Cao, L., and Zhang, X. (2019). Overexpression of B7-H3 in α-SMA-Positive Fibroblasts Is Associated With Cancer Progression and Survival in Gastric Adenocarcinomas. Front. Oncol. *9*, 1466. https://doi.org/10.3389/fonc.2019.01466.

43. Szot, C., Saha, S., Zhang, X.M., Zhu, Z., Hilton, M.B., Morris, K., Seaman, S., Dunleavey, J.M., Hsu, K.S., Yu, G.J., et al. (2018). Tumor stroma-targeted antibody-drug conjugate triggers localized anticancer drug release. J. Clin. Investig. *128*, 2927–2943. https://doi.org/10.1172/jci120481.

44. Abdollahi, A., and Folkman, J. (2010). Evading tumor evasion: current concepts and perspectives of anti-angiogenic cancer therapy. Drug Resist. Updat. *13*, 16–28. https://doi.org/10.1016/j.drup.2009.12.001.

45. Guo, S., Jiang, X., Mao, B., and Li, Q.X. (2019). The design, analysis and application of mouse clinical trials in oncology drug development. BMC Cancer *19*, 718. https://doi.org/10.1186/s12885-019-5907-7.

46. Breij, E.C.W., de Goeij, B.E.C.G., Verploegen, S., Schuurhuis, D.H., Amirkhosravi, A., Francis, J., Miller, V.B., Houtkamp, M., Bleeker, W.K., Satijn, D., and Parren, P.W.H.I. (2014). An antibody-drug conjugate that targets tissue factor exhibits potent therapeutic activity against a broad range of solid tumors. Cancer Res. *74*, 1214–1226. https://doi.org/10.1158/0008-5472.Can-13-2440.

47. Li, F., Emmerton, K.K., Jonas, M., Zhang, X., Miyamoto, J.B., Setter, J.R., Nicholas, N.D., Okeley, N.M., Lyon, R.P., Benjamin, D.R., and Law, C.L. (2016). Intracellular Released Payload Influences Potency and Bystander-Killing Effects of Antibody-Drug Conjugates in Preclinical Models. Cancer Res. *76*, 2710–2719. https://doi.org/10.1158/0008-5472.Can-15-1795.

48. Tian, H., Lyu, Y., Yang, Y.G., and Hu, Z. (2020). Humanized Rodent Models for Cancer Research. Front. Oncol. *10*, 1696. https://doi.org/10.3389/fonc.2020.01696.

49. Saber, H., Simpson, N., Ricks, T.K., and Leighton, J.K. (2019). An FDA oncology analysis of toxicities associated with PBD-containing antibody-drug conjugates. Regul. Toxicol. Pharmacol. *107*, 104429. https://doi.org/10.1016/j.yrtph.2019.104429.

50. Visintin, A., Knowlton, K., Tyminski, E., Lin, C.I., Zheng, X., Marquette, K., Jain, S., Tchistiakova, L., Li, D., O'Donnell, C.J., et al. (2015). Novel Anti-TM4SF1 Antibody-Drug Conjugates with Activity against Tumor Cells and Tumor Vasculature. Mol. Cancer Ther. *14*, 1868–1876. https://doi.org/10.1158/1535-7163.Mct-15-0188.

51. Rodig, S.J., Cheng, J., Wardzala, J., DoRosario, A., Scanlon, J.J., Laga, A. C., Martinez-Fernandez, A., Barletta, J.A., Bellizzi, A.M., Sadasivam, S., et al. (2012). Improved detection suggests all Merkel cell carcinomas harbor Merkel polyomavirus. J. Clin. Investig. *122*, 4645–4653. https://doi.org/10.1172/jci64116.

52. Bhatia, K., Goedert, J.J., Modali, R., Preiss, L., and Ayers, L.W. (2010). Merkel cell carcinoma subgroups by Merkel cell polyomavirus DNA relative abundance and oncogene expression. Int. J. Cancer *126*, 2240–2246. https://doi.org/10.1002/ijc.24676.

STAR★METHODS

KEY RESOURCES TABLE

REAGENT or RESOURCE	SOURCE	IDENTIFIER
Antibodies		
Goat polyclonal anti human CD276	R&D Systems	Cat#AF1027; RRID: AB_354546
Rabbit monoclonal anti mouse CD31	Cell Signaling Technology	Cat# 77699; Clone: D8V9E; RRID: AB_2722705
Mouse monoclonal anti human CD45	Ventana Medical Systems	Cat#790–4279; Clone: 2B11; RRID: N/A
Rabbit monoclonal anti human CD3	Ventana Medical Systems	Cat#790–4341; Clone: 2GV6; RRID: AB_2335978
Rabbit monoclonal anti human CD4	Ventana Medical Systems	Cat#790–4423; Clone: SP35; RRID:AB_2335982
Mouse monoclonal anti α-tubulin	Millipore Sigma	Cat#T9026; Clone: DM1A; RRID: AB_477593
Bacterial and virus strains		
None		
Biological samples		
Merkel cell carcinoma patient tumors	This paper (collected under relevant IRB protocols); Cooperative Human Tissue Network	https://www.chtn.org/
Formalin-fixed, paraffin-embedded sections of archival MCC patient tumors	This paper (collected under relevant IRB protocols); CHTN, UCI, VALBHS	N/A
Chemicals, peptides, and recombinant proteins		
m276-SL-PBD	Feng et al.[33]	N/A
Dual Endogenous Enzyme-Blocking Reagent	Agilent Technologies	Cat#S2003
Avidin/Biotin Kit	Vector Laboratories	Cat#SP2001
Critical commercial assays		
DNeasy Blood & Tissue Kit	Qiagen	Cat#69506
RNeasy Mini Kit	Qiagen	Cat#74104
High-Capacity cDNA Reverse Transcription Kit	Applied Biosystems	Cat#4368814
Cell Counting Kit - 8	Millipore Sigma	Cat#96992
Deposited data		
Western blot images	This paper; Mendeley Data	Figure 1; https://doi.org/10.17632/txxc39fwbj.1
Experimental models: Cell lines		
Patient derived MCC cell lines (MCC-5, MCC-9, MCC-16, MCC-21, MCC-22)	Generated in our lab	N/A
MKL-1 cell line	Gifted by Dr. Jurgen Becker (University Hospital Essen, Germany)	N/A
Experimental models: Organisms/strains		
Mouse: NOD.Cg-Rag1tm1Mom Il2rgtm1Wjl/SzJ (NRG)	The Jackson Laboratory	Strain #:007799 RRID:IMSR_JAX:007799
Mouse: NOD.Cg-Prkdcscid Il2rgtm1Wjl/SzJ (NSG)	The Jackson Laboratory	Strain #:005557 RRID:IMSR_JAX:005557
Mouse: Hu-NSG-CD34	The Jackson Laboratory	Strain #:705557

(*Continued on next page*)

Continued

REAGENT or RESOURCE	SOURCE	IDENTIFIER
Oligonucleotides		
Primer for LT3 (MCPyV detection) Forward 5′-TTGTCTCGCCAGCATTGTAG-3' Reverse 5′-ATATAGGGGCCTCGTCAACC-3′	Feng et al.[7]	N/A
Primer for LT1 (MCPyV detection) Forward 5′-TACAAGCACTCCACCAAAGC-3' Reverse 5′-TCCAATTACAGCTGGCCTCT-3′	Feng et al.[7]	N/A
qPCR primer and probe, LT3 (MCPyV detection) Forward 5′-TCGCCAGCATTGTAGTCTAAAAAC-3' Reverse 5′-CCAAACCAAAGAATAAAGCACTGA-3′ Probe FAM-AGCAAAAACACTCTC CCCACGTCAGACAG-BHQ	Rodig et al.[51]	N/A
qPCR primer and probe, Set9 (MCPyV detection) Forward 5′-TTAGCTGTAAGTTGTCTCGCC-3' Reverse 5′-CACCAGTCAAAACTTTCCCAAG-3′ Probe FAM-AAACACTCTCCCCACGTCAGACAG-BHQ	Rodig et al.[51]	N/A
qPCR primer and probe, SmallT (MCPyV detection) Forward 5′-GCAAAAAAACTGTCTGACGTGG-3' Reverse 5′-CCACCAGTCAAAACTTTCCCA-3′ Probe FAM-TATCAGTGCTTTATTCTT TGGTTTGGATTTCCTCCT-BHQ	Bhatia et al.[52]	N/A
MRPS2 (hs00211334_m1)	Life Technologies	Cat#4331182
CD276 (hs00987207_m1)	Life Technologies	Cat#4331182
Software and algorithms		
Graph Pad Prism v9	Graphpad	www.graphpad.com

EXPERIMENTAL MODEL AND SUBJECT DETAILS

Patient samples

Formalin-fixed, paraffin-embedded sections of archival MCC patient tumors were obtained from the Cooperative Human Tissue Network (CHTN), the University of California, Irvine (UCI), and Veterans Affairs Long Beach Healthcare System (VALBHS) after appropriate consent was obtained, under study protocols (UCI IRB HS #2020–6030 and VALBHS IRB #1619070) approved by local Institutional Review Boards (IRB) in accordance with local and federal regulations for human subject research. CHTN is an NCI-supported prospective collection service which provides deidentified human biospecimens to investigators, collected from routine procedures under protocols that are approved by local IRBs.

Fresh MCC tumor tissue used for the generation of PDX models was obtained from consenting MCC patients (Table S1) under study protocols approved by our local IRB (#1619070) and IACUC (#1710211).

Cell lines

Patient tumor derived MCC cell lines (coded as MCC-5, MCC-9, MCC-16, MCC-21, and MCC-22) were established in our lab under IRB-approved protocols (#131586 and #1619070, respectively) at the University of Arkansas for Medical Sciences and the VA Long Beach Healthcare System (VALBHS). MKL-1, a MCPyV-positive cell line from a male patient, was a kind gift from Dr. Jürgen Becker (University Hospital Essen, Germany). In brief, cell lines were established from patient tumor tissues, which had been surgically removed during routine care and were no longer needed for pathological diagnosis, collected by our study team after appropriate consent was obtained. MCC cell lines were authenticated against each respective primary MCC tumor by STR-profiling performed by Genetica (Laboratory Corporation of America; Burlington, NC); MKL-1 was compared against the associated STR profile in Cellosaurus (accession number CVCL_2600).

Animal participants

All *in vivo* studies were carried out under animal protocols (#1619104 and #1710211) approved by the Institutional Animal Care and Use Committee (IACUC) at the Veterans Affairs Long Beach Healthcare System (VALBHS), in accordance with laboratory animal care and use guidelines set by the Association for Assessment and Accreditation of Laboratory Animal Care (AAALAC) International and the American Veterinary Medical Association (AVMA). Male and female 6-to-8-week-old NOD *Rag* gamma mice (NRG) (Jackson Laboratory, strain #007799) were used to establish cell line-derived xenografts. Patient-derived xenograft models were established using

immunodeficient 6-to-8-week-old NOD *scid* gamma (NSG) female mice (Jackson Laboratory, strain #005557) and immunocompetent CD34$^+$ humanized NSG (huNSG) female mice (Jackson Laboratory, strain #705557), which were obtained from the youngest possible cohort (~18 weeks of age, due to the time required for human CD34$^+$ cell engraftment prior to availability for purchase). In accordance with USDA standards for laboratory animal husbandry and specific recommendations provided by the Jackson Laboratory (Bar Harbor, Maine) for these immunodeficient strains, mice were housed in stable groups in sterile microisolator caging with standard species-appropriate environmental enrichment, using strict barrier practices and aseptic technique to maintain pathogen-free colonies. In accordance with IACUC policy, federal law, and AVMA guidelines for the euthanasia of animals, mice were humanely euthanized upon reaching experimental or tumor endpoints.

METHOD DETAILS

Cell culture

Patient tumor derived MCC cell lines were maintained in suspension cultures in RPMI-1640 medium (#30–2001, American Type Culture Collection) supplemented with 10% fetal bovine serum, penicillin-streptomycin (100 U/mL), and L-glutamine (4mM) at 37°C with 5% CO_2. Media was refreshed every 48 h, and cells were split to maintain logarithmic growth. To determine the MCPyV status of each cell line, genomic DNA was isolated from cells using the DNeasy Blood & Tissue Kit (#69506, Qiagen) according to the manufacturer's instructions, and PCR and qRT-PCR were performed with primers used for MCPyV detection listed in the key resources table, as described in other studies.[7,51,52] PCR amplification using LT1 and LT3 primers was conducted using an iCycler Thermal Cycler (Bio-Rad) under standard cycling conditions, and PCR products were separated by electrophoresis on a 1.5% agarose gel and visualized under ultraviolet light. Quantitative real-time PCR was performed using LT3, Set9, and small T primers with the CFX96 Touch Real-Time PCR Detection System (Bio-Rad).

Quantitative real-time PCR

Total RNAs were extracted and purified using RNeasy Mini kit (#74104, Qiagen), and 1μg of total RNA was transcribed into cDNAs using the High-Capacity cDNA Reverse Transcription Kit (#4368814, Applied Biosystems) following manufacturers' protocols. The cDNAs were primed with TaqMan Gene Expression Assay primers (Assay ID hs00987207_m1, #4331182, Life Technologies) to examine CD276 expression, and triplicate reactions were run in the CFX96 Touch Real-Time PCR Detection System (Bio-Rad) following standard cycling conditions. Relative transcript expression was calculated by normalizing samples against the mitochondrial gene *MRPS2* using the ΔCt method.

Immunoblot analysis

Protein was purified from whole cell lysates in 1X radioimmunoprecipitation assay (RIPA) buffer (#R-0278, Millipore Sigma) containing cOmplete Mini EDTA-free protease inhibitor cocktail (#04693159001, Roche, obtained from Millipore Sigma). Whole cell protein lysates (20μg per lane) were resolved by 8% Tris-Glycine SDS polyacrylamide gel electrophoresis and transferred onto 0.45μm polyvinylidene difluoride membranes (#IPVH00010, Millipore Sigma) using Trans-Blot SD Semi-Dry Transfer Cell (#1703940, BioRad). Membranes were blocked with 5% fat-free milk (#70–6404, BioRad) in 1x Tris-buffered saline containing 0.1% Tween 20 (TBS-T) at room temperature for 1 h. To detect CD276 expression, membranes were incubated overnight at 4°C with a goat anti-CD276 polyclonal antibody (1:500, #AF1027, R&D Systems). As a loading control, α-tubulin was detected using a mouse anti-α-tubulin antibody (1:2500, #T9026, Millipore Sigma). Horseradish peroxidase (HRP)-conjugated secondary antibodies were applied to membranes for 1 h at room temperature. Membranes were visualized on autoradiography films (#BX57, Midwest Scientific) using the ECL kit (#WBULS0100, Millipore Sigma) following manufacturer's instructions.

Immunohistochemistry

Immunohistochemical (IHC) staining for CD276 on formalin-fixed, paraffin-embedded sections of MCC patient and xenograft tumor tissue began with deparaffinization and was followed by antigen retrieval in 1X citrate buffer (#H3300, Vector Laboratories) in a 98°C water bath. Sections were blocked for endogenous peroxidase and biotin using Dual Endogenous Enzyme Blocking Reagent (#S2003, Agilent Technologies) and the Avidin/Biotin Kit (#SP2001, Vector Laboratories), respectively, and further blocked with 1% casein (Roche #11096176001) in Tris-buffered saline (TBS). Goat anti-CD276 polyclonal antibody (1:100, #AF1027, R&D Systems) in 1% casein was applied to sections and incubated for 1 h at room temperature followed by overnight incubation at 4°C. Sections were treated with an avidin/biotin based peroxidase system (1:200, Vector Laboratories, #PK-6105) following manufacturer's instructions, and were subsequently incubated with DAB substrate (#SK-4105, Vector Laboratories) for signal detection. Slides were visualized, and positive CD276 staining was evaluated according to the intensity of tumor cell and tumor-associated vessel staining along with the percentage of immunoreactive cells. Similar to another study,[40] intensity of immunostaining was scored using the following criteria: 0, negative; 1, weak; 2, moderate; 3, strong. The percentage of immunoreactive cells was scored using the following criteria: 1, (0–10%); 2, (10–50%); 3, (51–100%). Final scores were calculated by multiplying the intensity and percentage of immunoreactive cells scores of the same section, with scores ranging from 0 to 9. Sections with a score of 4 or greater were defined as having strong expression.

For CD31 IHC, sections underwent deparaffinization followed by antigen retrieval in heated 1X citrate buffer (#H3300, Vector Laboratories) for 20 min, and were subsequently blocked with normal goat serum (#S1012, Vector Laboratories). Sections were incubated overnight with rabbit monoclonal anti-mouse CD31 primary antibody (1:100, Clone D8V9E, #77699, Cell Signaling Technology). Goat anti-rabbit secondary antibody (#MP-7451, Vector Laboratories) was applied for 30 min at room temperature, and signal was detected using a horseradish peroxidase (HRP) detection system with DAB as chromogen (#SK4105, Vector Laboratories).

IHC staining for human CD45, CD3, and CD4 was performed using the BenchMark ULTRA IHC/ISH system (Roche Diagnostics) following standard automated protocols. Slides were incubated with either anti-human CD45 antibody (pre-diluted, Clone 2B11, #790–4279, Ventana Medical Systems), anti-human CD3 antibody (pre-diluted, Clone 2GV6, #790–4341, Ventana Medical Systems), and anti-human CD4 antibody (pre-diluted, Clone SP35, #790–4423, Ventana Medical Systems). Signal detection was performed using an HRP-DAB system.

All stained sections were then visualized, and images were captured using a stereomicroscope with a digital camera (Discovery V12 and AxioCam; Carl Zeiss, Inc).

Cell viability and proliferation assay

Cell viability and proliferation was assessed using the Cell Counting Kit-8 (CCK-8) (#96992, Millipore Sigma) according to manufacturer's protocol. Cells were plated at a density of 1×10^5 cells/well in 96-well plates and incubated for 4 h at 37°C and 5% CO_2, after which they were exposed to serial concentrations of m276-SL-PBD for 72 h. CCK-8 reagent was added to each well at 10% of well volume and incubated for 2–4 h at 37°C. Optical density was measured at 450nm using a spectrophotometer. The dose-response curve was plotted normalized against cells treated with saline vehicle to calculate the half-maximal growth inhibitory dose (GI_{50}) and 95% confidence interval (CI95%) on GraphPad Prism 9.0 software.

Generation of MCC patient-derived xenograft (PDX) lineage

To generate MCC PDX lineages including the PDX-104 model utilized in this study, we obtained excess surgically removed tumor tissue from consenting MCC patients in accordance with the Declaration of Helsinki and relevant institutional guidelines for human studies, under study protocols approved by our local IRB (#1619070). Briefly, tumor tissues not needed for clinical diagnosis were obtained and processed by either sectioning into 2-4mm^3 pieces or preparing single-cell suspensions. Cells from non-necrotic tissues were subcutaneously implanted in 6-to-8-week-old immunodeficient NOD-scid-gamma (NSG) female mice (Jackson Laboratory, strain #005557); this initial engraftment was termed as "F_1" generation per standard parlance and allowed to grow until approaching tumor growth endpoint. Typically, successful F_1 engraftment can be observed within 4 months, although failure is not determined until at least 6 months after implantation/inoculation. Successfully established F_1 xenografts were biobanked and/or passaged into further mouse-to-mouse NSG cohorts, which were numbered consecutively as F_2, F_3, F_4 … generations. Representative xenografts were collected from each generational cohort and characterized by RT-PCR and immunohistochemistry, then compared against originating patient tumors. For the experiments described in this paper, we utilized the F_3 generation of our PDX-104 lineage, which exhibits classical MCC morphology and expresses classic MCC markers (data not shown).

m276-SL-PBD preclinical drug studies

All *in vivo* studies were carried out under IACUC-approved protocols in accordance with laboratory animal care and use guidelines set by AALAC, as well as all applicable local and federal laws. MCC CDX and PDX models were generated by subcutaneously inoculating MCC cells in mice, as follows: 2 x 10^7 MKL-1 cells in female NRG mice, 2 x 10^7 MCC-22 cells in male and female NRG mice, 3 x 10^7 MCC-5 cells in female NRG mice, and 2 x 10^7 PDX-104 cells in female immunodeficient NSG mice and female humanized $CD34^+$ NSG mice (Jackson Laboratory, strains #007799, #005557, and #705557, respectively). Tumor-bearing mice were randomly divided into treatment and control groups ($n \geq 5$ for each group) receiving m276-SL-PBD or saline vehicle. m276-SL-PBD was diluted in sterile phosphate buffered saline (PBS) and administered at 0.5 mg/kg via intraperitoneal injection every week for 4 weeks, whereas control mice received vehicle only. Relapsed xenografts began retreatment with 3 or 4 weekly doses of m276-SL-PBD (0.5 mg/kg) when tumor volumes reached approximately 500mm^3 in volume. Mice were monitored daily and tumors were measured using digital calipers. Tumor volume (TV) was calculated as L x W^2/2, where length (L) is the longer dimension and width (W) is the shorter dimension. In accordance with IACUC policy, endpoints for all *in vivo* studies were established as follows: (i) when experimental course is completed OR when tumor growth reaches 2cm in any dimension, whichever comes first, or (ii) if mice exhibit physiological or behavioral distress that cannot be alleviated, they are humanely euthanized.

QUANTIFICATION AND STATISTICAL ANALYSIS

Data are presented as the mean ± standard error of the mean (SEM) or standard deviation (SD). GraphPad Prism 9.0 was used for statistical analysis with the significance threshold was set to FDR = 0.05.